Accepted Manuscript

A highly sensitive fluorescent turn-on biosensor for glycoproteins based on boronic acid functional polymer capped Mn-doped ZnS quantum dots

Lifang Chang, Haocheng Wu, Xiwen He, Langxing Chen, Yukui Zhang

PII: S0003-2670(17)31086-3

DOI: 10.1016/j.aca.2017.09.037

Reference: ACA 235462

To appear in: *Analytica Chimica Acta*

Received Date: 13 June 2017

Revised Date: 13 September 2017

Accepted Date: 15 September 2017

Please cite this article as: L. Chang, H. Wu, X. He, L. Chen, Y. Zhang, A highly sensitive fluorescent turn-on biosensor for glycoproteins based on boronic acid functional polymer capped Mn-doped ZnS quantum dots, *Analytica Chimica Acta* (2017), doi: 10.1016/j.aca.2017.09.037.

This is a PDF file of an unedited manuscript that has been accepted for publication. As a service to our customers we are providing this early version of the manuscript. The manuscript will undergo copyediting, typesetting, and review of the resulting proof before it is published in its final form. Please note that during the production process errors may be discovered which could affect the content, and all legal disclaimers that apply to the journal pertain.

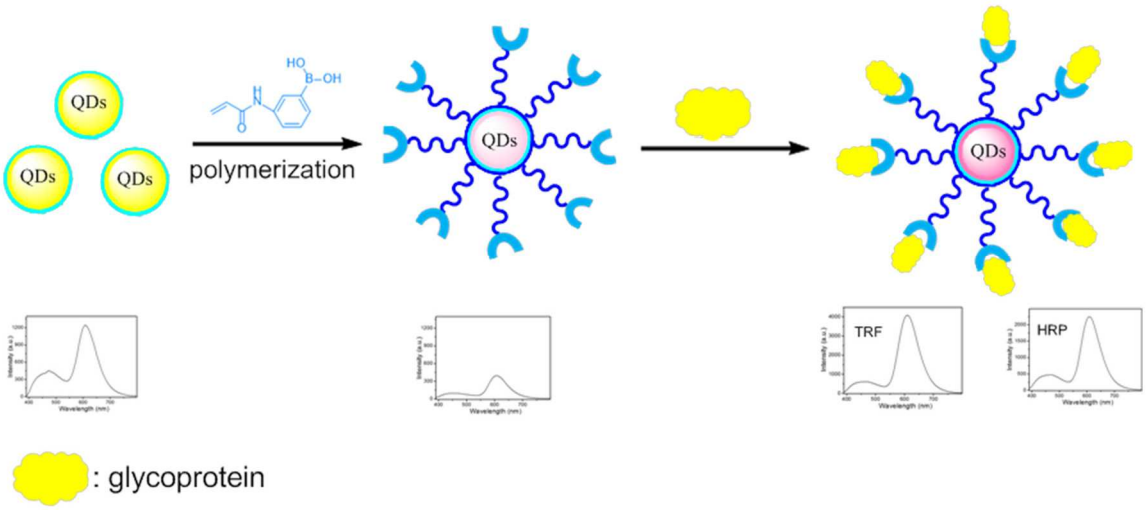

ACCEPTED MANUSCRIPT

ACCEPTED MANUSCRIPT

A highly sensitive fluorescent turn-on biosensor for glycoproteins based on boronic acid functional polymer capped Mn-doped ZnS quantum dots

Lifang Chang [a], *Haocheng Wu* [a], *Xiwen He* [a], *Langxing Chen* [a,b]* and *Yukui Zhang* [a,c]

[a]Research Center for Analytical Sciences, College of Chemistry, Tianjin Key Laboratory of Biosensing and Molecular Recognition, State Key Laboratory of Medicinal Chemical Biology, Nankai University, Tianjin 300071, China

[b]Collaborative Innovation Center of Chemical Science and Engineering (Tianjin), Tianjin 300071, China

[c]Dalian Institute of Chemical Physics, Chinese Academy of Sciences, Dalian 116011, China

Email: 1120140194@mail.nankai.edu.cn (L. F. Chang); 1330343202@qq.com (H. C. Wu); xiwenhe@nankai.edu.cn (X. W. He); lxchen@nankai.edu.cn (L. X. Chen), fax: +86-22-23502458; phone: +86-22-23505091; ykzhang@dicp.ac.cn (Y. K. Zhang)

ACCEPTED MANUSCRIPT

ABSTRACT: A simple fluorescence turn-on sensor has been designed for the highly sensitive detection of glycoproteins on the basis of boronic acid functional polymer capped Mn-doped ZnS quantum dots (QDs@MPS@AAPBA). In the absence of glycoproteins, the fluorescence emission intensity of the QDs@MPS@AAPBA was relatively weaker due to the effective electronic transfer from the QDs to the boron moieties on its surface. While the glycoproteins were introduced into the system, an obvious fluorescence enhancement was observed. It was attributed to the boron moieties covalent binding glycans of the glycoproteins resulting in the electronic transfer process being inhibited. Under the optimal conditions, this fluorescent probe not only could be applied in a wide pH range of 5.0-9.0, but also the binding constants and detection limits of the QDs@MPS@AAPBA for horseradish peroxidase (HRP) and transferrin (TRF) were up to 7.23×10^{6} M^{-1}, 1.53×10^{7} M^{-1} and 1.44×10^{-10} M, 3.36×10^{-10} M, respectively. Finally, this proposed method has also been utilized for the TRF determination in serum without any complicated pretreatment and the recovery was in the range of 95.7%-103.0%. As a result, it is promising for application on the glycoproteins detection in complex biological samples.

Keywords: Mn-doped ZnS quantum dots; fluorescent sensor; turn-on; boronate affinity; glycoproteins

ACCEPTED MANUSCRIPT

1. Introduction

Glycoproteins, composed of glycosyl (oligosaccharide chains) and proteins, play an important role in biological process such as molecular recognition, cellular immune response and cell regulation [1]. The abnormal expression of glycoproteins is associated with various diseases such as hepatocellular carcinoma, Alzheimer's disease and cancer and so on, so a large variety of glycoproteins are of great significance in clinical diagnostics [2]. For example, α-fetoprotein-L3, MUC1 mucin and α1-acid glycoprotein are often employed as the biomarkers for liver cancer, breast cancer and neoplasia, respectively [3-6]. However, owing to glycoprotein biomarkers with the low concentrations in crude biological samples as well as high background of interfering species with high abundance in the sample matrix, the limited concentrations are hard to be efficiently detected. As a consequence, highly selective and sensitive analytical approaches for the specific detection of glycoprotein biomarkers in real-world applications have driven researchers more and more attractive. Fluorescence sensing has been attracted much attention due to its fast response, high sensitivity and selectivity [7,8]. Recently, Chen et al. developed a fluorescence turn-off system based on CdTe QDs for detecting the enzymatic activity of α-L-fucosidase with the detection limit of 0.01 U L^{-1} [9]. Gao et al. reported a fluorescent probe based on energy transfer between $CuInS_2$ QDs-Con A and rhodamine B-NH_2-glu for the detection of TRF and glucose oxidase (GOx) [10]. Zhang et al. described a novel fluorescence probe based on increased polarity of C-B bonds for monitoring hydrogen peroxide in living cells [11]. Li et al. synthesized a fluorescence turn-off sensor based on 3-aminophenylboronic acid functionalized copper nanoclusters for the detection of glycoproteins [12]. Tang's groups reported the fluorescence

nanosensors based on molecularly imprinted polymers (MIPs) and boronate affinity for monitoring glycoproteins [13,14]. In spite of high selectivity, not only most of the biological materials (lectins, antigens et al.) are expensive but lack of fluorescence turn-on probe is observed. Therefore, a simple and low-cost fluorescence turn-on sensor with a more sensitive and selective detection of glycoproteins is highly desirable.

It is well-known that boronic acids can reversibly covalently bind sugars and glycoproteins containing *cis*-diols via forming five or six membered cyclic esters in an alkaline solution. However, the cyclic esters will dissociate when the ambient pH is switched to acidic [15,16]. In recent years, boronate affinity has gained an increasing attention due to its significant applications in glycoproteins sensing [16-21] and separating [22-25]. As glycoproteins and sugars are valuable enough in biology and clinic, boronate affinity-mediated fluorescent sensors are of great importance. In comparison with other fluorescent probes, boronic acid functionalized fluorescent probes take advantages of better water solubility [26], higher selectivity [27,28] and sensitivity [29]. Recently, boronic acid functioned fluorescent sensors have been reported in a few papers. Anslyn's group designed and synthesized a boronic acid porphyrin receptor for ginsenoside sensing [30]. Zhou's group reported phenylboronic acid modified CdTe/ZnTe/ZnS Quantum Dots for intracellular glucose probing [31]. Strano's group described a library of 30 boronic acid derivatives with forming complexes with sodium cholate suspended single-walled carbon nanotubes (SWNTs) to reversibly report glucose binding via a change in SWNT fluorescence [32]. Xia's group fabricated boronic acid functionalized carbon dots by one-step strategy for fluorescent blood sugar sensing [33]. Jiang's group prepared a fluorescence probe based on

boronic acid functionalized aza-bodipy for the analysis of glucose in whole blood [34]. Despite the significant advances, fluorescence probes based on boronate affinity for the analysis and detection of glycoproteins are still few till now.

Previously, we had designed and prepared a fluorescence turn-on biosensor based on mercaptophenylboronic acid (MBA) capped Mn^{2+}-ZnS QDs for the sensitive determination of transferrin (TRF), and the limit of detection was about 5.69 nM [35]. Inspired by this observation, we have synthesized boronic acid functional polymer capped Mn-doped ZnS QDs (QDs@MPS@AAPBA) for the fluorescent detection of glycoproteins in this work (Scheme 1). Compared with our previous report, boronic acid polymer, designed as the fluorescent receptor, was expected to induce a more obvious fluorescence enhancement due to its more boron moieties in the presence of glycoproteins. Herein, transferrin and horseradish peroxidase, as models of glycoproteins, were introduced to evaluate sensitivity and selectivity of the probe. Transferrin, a molecular mass of 77 kDa, is a single polypeptide chain glycoprotein of 670-700 amino acids, and is responsible for iron transport in serum [36,37]. Horseradish peroxidase, a glycoprotein with molecular mass of 40 kDa, is composed of colourless zymoprotein and brown ferriporphyrin [38].

2. Experimental

2.1. Materials

Horseradish peroxidase (HRP) (MW-40 kDa), transferrin (TRF) (MW-77 kDa), bovine serum albumin (BSA) (MW-68 kDa), cytochrome C (CYT) (MW-12 kDa), and lysozyme (LYZ) (MW-14 kDa) were purchased from Sigma-Aldrich (USA). α-D-gluocose and

α-D-fructose were purchased from Heowns Biochem LLC (Tianjin, China). Zinc sulfate hepahydrate ($ZnSO_4 \cdot 7H_2O$), manganese sulfate tetrahydrate ($MnSO_4 \cdot 4H_2O$), sodium sulfide nonahydrate ($NaS \cdot 9H_2O$), sodium chloride (NaCl), magnesium chloride ($MgCl_2$), calcium chloride ($CaCl_2$), potassium chloride (KCl), sodium bicarbonate ($NaHCO_3$) and ammonium hydroxide ($NH_3 \cdot H_2O$) were all obtained from Tianjin Chemical Reagent Company (Tianjin, China), which were used directly without further purification. Mercaptopropyltrimethoxysilane (MPTS), (3-(methacryloxy)propyl)trimethoxysilane (MPS), 3-aminophenylboronic acid (APBA) and acrylchloride were obtained from Tokyo Chemical Industry (Japan). Other reagents were of analytical grade or better. Ultrapure water was prepared with a Milli-Q water purification system (Millipore, Milford, MA, USA).

2.2. *Instruments and characterizations*

The crystal structure of prepared QDs@MPS@AAPBA was determined by an X-ray diffractometer (XRD). The XRD pattern of each sample was recorded with a Shimadzu (Japan) D/Max-2500 diffractometer, using a monochromatized X-ray beam with nickel-filtered Cu Kα radiation. The XRD patterns were collected in the range of $3^o < 2\theta < 80^o$ with a dwelling time of 2 s and a scan rate of 6.0^o min^{-1}. The size and morphology of the QDs@MPS and QDs@MPS@AAPBA were measured by a JEOL JEM-2100 transmission electron microscope (TEM). The QDs sample dispersed in ultrapure water was cast onto a carbon-coated copper grid sample holder followed by evaporation at room temperature. X-ray photoelectron spectroscopy (XPS) measurements were performed with an ESCALAB 250 spectrometer (Thermo-VG Scientific) with ultrahigh vacuum generators. The responses with TRF and HRP of the prepared QDs@MPS@AAPBA were obtained by using a FL-4500

spectrophotometer (Shimadzu, Japan). Fourier transform infrared (FT-IR) spectra (4000-400 cm^{-1}) in KBr were recorded using the AVATAR 360 FT-IR spectrophotometer (Nicolet, Waltham, USA).

2.3. Synthesis of MPTS modified Mn-doped ZnS QDs (QDs@MPTS)

The synthetic routes of MPTS-capped Mn-doped ZnS QDs were similar to the literature mentioned previously [39]. $ZnSO_4 \cdot 7H_2O$ (3.6 g, 12.5 mmol) and $MnSO_4 \cdot 4H_2O$ (0.22 g, 1.3 mmol) were dissolved in 40 mL ultrapure water in 100 mL three-necked flask, stirred under argon at room temperature for 10 min, and then added 10 mL aqueous solution containing of $Na_2S \cdot 9H_2O$ (3.0 g, 12.5 mmol). After stirring for 30 min, 10 mL absolute ethanol containing of 200 μL MPTS was added into the solution and then kept stirring for 20 h. Finally, the product was precipitated with absolute ethanol, separated by centrifuging, washed with ultrapure water and absolute ethanol for three times, and dried in vacuum for 8 h.

2.4. Synthesis of MPS modified Mn-doped ZnS QDs (QDs@MPS)

The MPS modified QDs were synthesized referring to the procedure described in the paper [40]. To a 100 mL round-bottomed flask, QDs@MPTS (0.2 g) were monodispersed in the mixture of 50 mL H_2O-ethanol (v/v, 10 mL/40 mL) with ultrasound about 30 min, and then $NH_3 \cdot H_2O$ (1.5 mL) and MPS (0.5 mL) were added. The mixture was kept under magnetic stirring for 24 h at 60 ^oC. At last, the obtained mixture was separated by centrifuging and washed with ethanol to remove the excess MPS and then dried in a vacuum oven at 40 °C overnight.

2.5. Synthesis of boronic acid polymer functionalized QDs (QDs@MPS@AAPBA)

The core-shell structured QDs@MPS@AAPBA was prepared via a one-step sol-gel

polymerization technique. Typically, QDs@MPS (100 mg) was monodispersed in methanol (40 mL) in a dried 100 mL single-necked flask. Then 100 mg 3-acrylaminophenylboronic acid (AAPBA) and 40 mg 2,2′-azodiisobutyronitrile (AIBN) were added to the reactor. The mixture was kept under magnetic stirring for 24 h at 60 ^{o}C. Finally, the obtained QDs@MPS@AAPBA composites were collected by centrifuging separation and washed with methanol three times in order to eliminate excess monomers and oligomers, and then dried at 40 °C in a vacuum oven.

2.6. QDs@MPS@AAPBA for glycoproteins analysis

For determination of glycoproteins, QDs@MPS@AAPBA (50 mg) was dispersed in 20 mM phosphate buffered saline (PBS) (pH 9.0) and diluted to 500 mL volumetric flask. Subsequently, various concentrations of TRF from 0.0 to 5.0 μM and HRP from 0.0 to 2.0 μM separately in 1 mL 100 mg L^{-1} QDs@MPS@AAPBA solution and incubated for 2 h in an incubator shaker at room temperature. The solutions were analyzed by fluorescence spectrophotometer with the excited wavelength of 310 nm, the voltage of 950 V, and slit 10, 10.

2.7. Selectivity of QDs@MPS@AAPBA to glycoproteins determination

HRP, BSA, LYZ, CYT, α-D-glucose, α-D-fructose and α-D-mannose were selected as analogues to evaluate the selectivity of QDs@MPS@AAPBA to glycoproteins. Each of QDs@MPS@AAPBA solutions (1 mL 100 mg L^{-1}) in 2 mL tubes, containing TRF (1.0 μM), HRP (1.0 μM) or other analogues (10.0 μM), were incubated for 2 h at room temperature, and then characterized by fluorescent method. The responses to glycoproteins and the analogues on QDs@MPS@AAPBA were compared.

2.8. Anti-interference ability of QDs@MPS@AAPBA for TRF in a simulated physiological condition

QDs@MPS@AAPBA solutions in the presence of 1.0 μM TRF and 10.0 μM its interfering substances which all coexist in human blood, were incubated for 3 h at room temperature, respectively. Competition events were also monitored by fluorescent spectrophotometer, and all tests were conducted in triplicate.

2.9. Determination of TRF in serum sample

Fetal bovine serum (FBS) was selected for spiked sample analysis. First, 1 μL FBS was diluted 100 times with 20 mM phosphate buffer containing 100 mg L^{-1} QDs@MPS@AAPBA (pH 9.0). Then 0.2-0.8 μM standard solutions of TRF were added to 1 mL of diluted FBS solution in 2 mL plastic tubes, respectively. The tubes were shaken on a rotator for 2 h at room temperature. Finally, the solutions were directly analyzed by fluorescent spectrophotometer.

3. Results and discussion

3.1. Preparation and Characterization of QDs@MPS@AAPBA

QDs@MPS@AAPBA sensor was constructed based on that the Mn-doped ZnS QDs as the core which plays a role in luminescent antennae for recognition signal amplification and optical readout, while the polymer layer as the shell provides selectivity of glycoproteins and prevents interfering molecules from being close to the QDs core. In this work, we have synthesized the QDs@MPS@AAPBA in Scheme 1.

The size and morphology of the obtained QDs@MPS and QDs@MPS@AAPBA under the experimental condition was characterized by TEM. Fig. 1A revealed that the silica layer

was successfully coated on the surface of Mn-ZnS QDs. Fig. 1C showed the morphology of QDs@MPS after boronic acid polymer modification. The silica and boronic acid polymer shell resulted in the morphology difference between QDs@MPS and QDs@MPS@AAPBA (Fig.1A, 1C). It is clearly observed that the crystal lattice fringe with a spacings of 0.279 nm from the HRTEM images of QDs@MPTS and QDs@MPS@AAPBA (Fig. 1B, 1D) , which can be assigned to the (111) plane of Mn doped ZnS quantum dots and the diameter of Mn-ZnS QDs is about 3.3 nm. The crystal structure of lattice Mn-ZnS QDs kept unchangeable during the silica and polymerization modification.

The XRD pattern of all Mn-doped ZnS QDs exhibited a cubic structure with peaks for (111), (220) and (311) planes in Fig. 2A. It is suggested that the crystalline lattices of Mn-doped ZnS QDs are pretty integrated. FT-IR spectra of QDs, QDs@MPS and QDs@MPS@AAPBA are exhibited in Fig. 2B. As for the QDs@MPS, the strong band at 1114 cm^{-1} is Si–O–Si stretching vibration, 3423 cm^{-1} is –OH stretching vibration, and 1645 cm^{-1} is the C=C deformation vibration. As for the QDs@MPS@AAPBA, the peak at 1300 cm^{-1} is attributed to the characteristic band of B–O, 2925 cm^{-1} is C–H stretching vibration, 1708 cm^{-1} is C–O stretching vibration and 1400 cm^{-1} is C–N stretching vibration. The disappearance of 1645 cm^{-1} revealed that the polymerization reaction has happened. The XPS spectra of the as-prepared QDs@MPS@AAPBA were recorded to analyze the chemical compositions and gain more structure information. As can be seen from Fig. 2C, the elements of Zn, S, N, C, Si, Mn, B and O could be observed. In the high-resolution B 1s spectrum of QDs@MPS@AAPBA (Inset in Fig. 2C), the peak at 188 eV is attributed to the B-O bond. In Fig. 2D, the fluorescence spectra of QDs@MPS@AAPBA overall exhibit a

weak blue and short-lived emission centre at 450 nm due to the defect-related emission of the ZnS QDs, and a strong orange and long-lived emission around 610 nm owing to the dopant-related Mn^{2+} doped ZnS QDs. However, it is obvious that the fluorescent emission intensity of QDs@MPS@AAPBA dramatically decreases. Besides, it is observed significantly that the fluorescence of QDs turns from orange to pink after polymerization of AAPBA.

3.2. Fluorescence sensing of glycoproteins using QDs@MPS@AAPBA

To confirm the ability of the described sensor to sensitively detect target glycoproteins and the interactions between QDs@MPS@AAPBA and glycoproteins, TRF and HRP as the models of glycoproteins were conducted in all experiments. As shown in Fig. 3A, the fluorescent spectra of QDs@MPS@AAPBA in the presence of a series of different concentrations of TRF were measured, and the results displayed a significant variation of fluorescence emission in the presence of 0.0 μM-3.0 μM TRF. It is observed that the fluorescence intensity increased gradually as the concentrations of TRF increase. The fluorescence changes mechanism of biosensor for determination of glycoproteins can be described as follow. The boronic acid groups on the surface of the quantum dots are electron deficient. Therefore, the electrons in the excited state of the quantum dots jump into the empty orbit of the boronic acid groups instead of returning to the ground state, which weakens the intensity of fluorescence emission. After binding with the cis-diols groups in the TRF / HRP, the boronic acid groups changed from sp^2 to sp^3 hybrid orbital with a octet structure which blocked the electron transfer from quantum dots to boronic acid groups and caused enhancement of fluorescence intensity. As inset in Fig. 3A depicted, when the

concentration of TRF was up to 1.0 μM, the fluorescence emission intensity reached the peak with a significant enhancement about 9.5-fold within 30 min (Fig. S1, Supplementary Material). Fig. 3B depicted that the linear range was from 0.4 μM to 0.9 μM for TRF detection, and the binding constant (*k*) between QDs@MPS@AAPBA and TRF was calculated to be 1.53×10^{7} M^{-1}, according to the equation of $\Delta F/F_0 = k\, C_{TRF}$ [41], where C_{TRF} was the concentration of TRF in QDs@MPS@AAPBA solution, $\Delta F = F - F_0$, and F and F_0 were the fluorescent intensity of QDs@MPS@AAPBA in the presence and absence of TRF. Similarly, the fluorescence emission of QDs@MPS@AAPBA in presence of HRP from 0.0 μM to 2.0 μM was also increased around 5.0-fold in Fig. 3C and its inset, the linear range of HRP determination was 0.3-0.7 μM shown in Fig. 3D, and the binding constant (*k*) between QDs@MPS@AAPBA and HRP was estimated to be 7.23×10^{6} M^{-1}. The good combination between the boronate of QDs@MPS@AAPBA and sialylated glycans of TRF or HRP forming five or six membered lactone ring is based on the mechanism of boronate affinity in alkaline conditions. The limit of detection of TRF and HRP from the standard deviation three times corresponding to the blank sample detection, was measured to be 1.44×10^{-10} M and 3.36×10^{-10} M, respectively (Fig. S2, Supplementary Material). To the best of our knowledge, the detection limit in this work is 10 to 200 times lower than those of fluorescent probes (Table 1) [12, 21, 35, 42, 43]. The fluorescence emission of QDs@MPS@AAPBA in the absence of TRF or HRP, is relatively lower due to electron deficiency of the QDs composite induced by the electron transfer from the QDs to the boron moieties. When the boron moieties of QDs@MPS@AAPBA coordinating with TRF or HRP, becomes negatively charged, the electron transfer between the QDs and the boron moieties is blocked, leading to

a loss of quenching efficiency and an obvious enhancement in fluorescence intensity.

3.3. Selectivity of the QDs@MPS@AAPBA

To identify the selectivity of the QDs@MPS@AAPBA for the glycoproteins, compared with sugars such as glucose and fructose (*cis*-diol-containing compounds), and non-glycosylated proteins such as BSA, CYT and LYZ, the fluorescent signals of detection TRF and HRP were conducted in 20 mM PBS (pH 9.0). Fig. 4A demonstrated that fluorescence emission of QDs@MPS@AAPBA in presence of 1.0 μM for either TRF or HRP exhibited an obvious turn-on about 9.5-fold and 5.0-fold, respectively. However, there was just slight enhancement in the presence of 10 μM for non-glycosylated proteins and also a little decrease for 100 μM sugars on the fluorescent emission of QDs@MPS@AAPBA. Although there are definite interactions between the fructose and boron moieties, the steric hindrance of fructose is small, which can cause aggregation-induced fluorescence quenching after binding with QDs@MPS@AAPBA. As a result, unlike those glycoproteins, the sugars did not induce the fluorescent emission enhancement of QDs@MPS@AAPBA. As a result, it revealed that QDs@MPS@AAPBA had a high specificity to glycoproteins. Besides, the anti-interference ability of QDs composites to glycoproteins was also employed in the presence of non-glycosylated proteins (BSA, CYT and LYZ) or some relevant particles (glucose, Na^+, K^+, Ca^{2+}, Mg^{2+}, Cl^-, HCO_3^-) which mainly exist in human serum. It is suggested that there existed no influence on the detection of TRF even at relatively high concentrations except Na^+ and Cl^- in Fig. 4B. The fluorescence intensity of the QDs@MPS@AAPBA in presence of TRF decreased to some extent when high concentration of Na^+ (142 mM) or Cl^- (100 mM) was being introduced into the solution. The

277 weakened fluorescence emission of QDs@MPS@AAPBA can be attributed to not only
278 interactions between the ligands on the surface of QDs@MPS@AAPBA and ions, but also
279 the Coulomb potential of ions displacing the wave functions of the electron and hole
280 confined inside the QDs [44,45]. As a result, it indicates that QDs@MPS@AAPBA can be
281 applied to detect the level of TRF in human serum, which is of great importance to the
282 disease diagnosis.

283 The influence of pH on fluorescent response to the QDs@MPS@AAPBA in the presence
284 or absence of TRF was also assessed. As shown in Fig. 5, over a pH range of 5.0-9.0, no
285 significant fluorescence changes were observed for QDs@MPS@AAPBA alone, while there
286 was an obvious fluorescent intensity enhancement in the presence of 1.0 μM TRF. The result
287 indicated that the QDs@MPS@AAPBA can be utilized as an optical biosensor for the
288 detection of glycoproteins within a wide pH span of 5.0-9.0.

289 *3.4. QDs@MPS@AAPBA for selective detection of TRF in serum*

290 To demonstrate the potential application of QDs@MPS@AAPBA to the complex
291 biological samples, the detection of TRF in fetal bovine serum (FBS) by the as-prepared
292 QDs@MPS@AAPBA was conducted and the results were depicted in Table 2. The
293 concentrations of TRF (0.5 to 0.8 μM) were spiked into the serum diluted to 100-fold, and
294 the recovery was 95.8%-103.0%. The results suggested that this sensor has great potential
295 for determining the glycoproteins concentration in complex biofluids.

296

297 **4. Conclusion**

298 In this work, a new fluorescent turn-on sensor for glycoproteins based on

299 QDs@MPS@AAPBA has been fabricated. The use of boronate-affinity interaction shows
300 good selectivity and sensitivity for the detection of glycoproteins, and it has the potential for
301 the determination of glycoproteins in complex biological samples without interference from
302 background and other components. The limit of detection of TRF or HRP is lower down to
303 be 10^{-10} M in aqueous solution, and the QDs@MPS@AAPBA can be utilized as an optical
304 biosensor for the detection of glycoproteins within a wide pH span of 5.0-9.0. These results
305 demonstrate that QDs@MPS@AAPBA is promising for application to serum using
306 fluorescent detection.

307 **Acknowledgements**

308 This work was supported by the National Natural Science Foundation of China (No.
309 21475067, 21275080) and the Natural Science Foundation of Tianjin (No.
310 15JCYBJC20600).

311

ACCEPTED MANUSCRIPT

312 **References**

313 [1] P.M. Rudd, T. Elliott, P. Cresswell, I.A.Wilson, R.A. Dwek, Glycosylation and the immune system,
314 Science 291 (2001) 2370-2376.

315 [2] H. Narimatsu, H. Sawaki, A. Kuno, H. Kaji, H. Ito, Y.A. Ikehara, Strategy for discovery of cancer
316 glyco-biomarkers in serum using newly developed technologies for glycoproteomics, Febs. J. 277
317 (2010) 95-105.

318 [3] M. Okuyama, H. Ueno, Y. Kobayashi, H. Kawagishi, D. Takahashia, K. Toshima, Target-selective
319 photo-degradation of AFP-L3 and selective photo-cytotoxicity against HuH-7 hepatocarcinoma
320 cells using an anthraquinone-PhoSL hybrid, Chem. Commun. 52 (2016) 2169-2172.

321 [4] P. Wu, Y. Gao, H. Zhang, C.X. Cai, Aptamer-guided silver-gold bimetallic nanostructures with
322 highly active surface-enhanced raman scattering for specific detection and near-infrared
323 photothermal therapy of human breast cancer cells, Anal. Chem. 84 (2012) 7692-7699.

324 [5] K. Kakehi, M. Kinoshita, D. Kawakami, J. Tanaka, K. Sei, K. Endo, Y. Oda, M. Iwaki, T. Masuko,
325 Capillary electrophoresis of sialic acid-containing glycoprotein. Effect of the heterogeneity of
326 carbohydrate chains on glycoform separation using an α1-acid glycoprotein as a model, Anal. Chem.
327 73 (2001) 2640-2647.

328 [6] E. Giménez, M. Balmaña, J. Figueras, E. Fort, C. de Bolós, V. Sanz-Nebot, R. Peracaula, A. Rizzi,
329 Quantitative analysis of N-glycans from human alfa-acid-glycoprotein using stable isotope labeling
330 and zwitterionic hydrophilic interaction capillary liquid chromatography electrospray mass
331 spectrometry as tool for pancreatic disease diagnosis, Anal. Chim. Acta 866 (2015) 59-68.

332 [7] W. Zhang, J.Q. Kang, P. Li, H. Wang, B. Tang, Dual signaling molecule sensor for rapid detection
333 of hydrogen sulfide based on modified tetraphenylethylene, Anal. Chem. 87 (2015) 8964−8969.

[8] W. Zhang, W. Liu, P. Li, J.Q. Kang, J.Y. Wang, H. Wang B. Tang, Reversible two-photon fluorescent probe for imaging of hypochlorous acid in live cells and in vivo, Chem. Commun. 51 (2015) 10150-10153.

[9] Z.Z. Chen, X.L. Ren, X.W. Meng, Y.Q. Zhang, D. Chen, F.Q. Tang, Novel fluorescence method for detection of α-l-fucosidase based on CdTe quantum dots, Anal. Chem. 84 (2012) 4077-4082.

[10] X. Gao, D. Li, Y. Tong, D. Ge, Y.W. Tang, D.F. Zhang, J.R. Li, Highly sensitive fluorescence detection of glycoprotein based on energy transfer between $CuInS_2$ QDs and rhodamine B, Luminescence 30 (2015) 1389-1394.

[11] W. Zhang, W. Liu, P. Li, F. Huang, H. Wang, B. Tang, Rapid-response fluorescent probe for hydrogen peroxide in living cells based on increased polarity of C−B bonds, Anal. Chem. 87 (2015) 9825-9828.

[12] X.G. Li, F. Zhang, Y. Gao, Q.M. Zhou, Y. Zhao,Y. Li, J.Z. Huo, X.J. Zhao, Facile synthesis of red emitting 3-aminophenylboronic acid functionalized copper nanoclusters for rapid, selective and highly sensitive detection of glycoproteins, Biosens. Bioelectron. 86 (2016) 270-276.

[13] W. Zhang, W. Liu, P. Li, H.B. Xiao, H. Wang, B. Tang, A Fluorescence nanosensor for glycoproteins with activity based on the molecularly imprinted spatial structure of the target and boronate affinity, Angew. Chem. Int. Ed. 53 (2014) 12489-12493.

[14] W. Zhang, J.Q. Kang, P. Li, L. Liu, H. Wang B. Tang, Two-photon fluorescence imaging of sialylated glycans in vivo based on a sialic acid imprinted conjugated polymer nanoprobe, Chem. Commun. 52 (2016) 13991-13994.

[15] R. Nishiyabu, Y. Kubo, T.D. James, J.S. Fossey, Boronic acid building blocks: tools for sensing and separation, Chem. Commun. 47 (2011) 1106-1123.

[16] M.J. Edgeworth, J.J. Phillips, D.C. Lowe, A.D. Kippen, D.R. Higazi, J.H. Scrivens, Global and local conformation of human IgG antibody variants rationalizes loss of thermodynamic stability, Angew. Chem. Int. Ed. 54 (2015) 15156-15159.

[17] R. Nishiyabu, Y. Kubo, T.D. James, J.S. Fossey, Boronic acid building blocks: tools for self assembly, Chem.Commun. 2011, 47, 1124-1150.

[18] J. Lee, H. Park, M. Kim, Y. Lee, S.J. Byun, S. Lee, M.H. Kwon, Functional stability of 3D8 scFv, a nucleic acid-hydrolyzing single chain antibody, under different biochemical and physical conditions, Int. J. Pharm. 496 (2015) 561-570.

[19] J. Ye, Y. Chen, Z. Liu, A boronate affinity sandwich assay: an appealing alternative to immunoassays for the determination of glycoproteins, Angew. Chem. Int. Ed. 53 (2014) 10386-10389.

[20] X.D. Bi, D.J. Li, Z. Liu, Pattern recognition of monosaccharides via a virtual lectin array constructed by boronate affinity-based pH-featured encoding, Anal. Chem. 87 (2015) 4442-4447.

[21] J.R. Wei, Y.L. Ni, W. Zhang, Z.Q. Zhang, J. Zhang, Detection of glycoprotein through fluorescent boronic acid-based molecularly imprinted polymer, Anal. Chim. Acta 960 (2017) 110-116.

[22] H.Y. Li, Z. Liu, Recent advances in monolithic column-based boronate-affinity chromatography, Trends Anal. Chem. 37 (2012) 148-161.

[23] H.Y. Nie, Y. Chen, C.C. Lü, Z. Liu, Efficient selection of glycoprotein-binding DNA aptamers via boronate affinity monolithic capillary, Anal. Chem. 85 (2013) 8277-8283.

[24] W.X. Chen, Y.F. Cheng, B.H. Wang, Pellasoren: structure elucidation, biosynthesis, and total synthesis of a cytotoxic secondary metabolite from sorangium cellulosum, Angew. Chem. Int. Ed. 51 (2012) 5293-5295.

[25] L.X. Li, Z.N. Xia, J. Pawliszyn, Selective extraction and enrichment of glycoproteins based on boronate affinity SPME and determination by CIEF-WCID, Anal. Chim. Acta 886 (2015) 83-90.

[26] M. Jamkratoke, V. Ruangpornvisuti, G. Tumcharern, T. Tuntulani, B. Tomapatanaget, A-D-A sensors based on naphthoimidazoledione and boronic acid as turn-on cyanide probes in water, J. Org. Chem. 74 (2009) 3919-3922.

[27] X. Zhang, L.N. Chi, S.M. Ji, Y.B. Wu, P. Song, K.L. Han, H.M. Guo, T.D. James, J.Z. Zhao, Rational design of d-PeT phenylethynylated-carbazole monoboronic acid fluorescent sensors for the selective detection of r-hydroxyl carboxylic acids and monosaccharides, J. Am. Chem. Soc. 131 (2009) 17452-17463.

[28] X.M. Gao, Y.L. Zhang, B.H. Wang, A highly fluorescent water-soluble boronic acid reporter for saccharide sensing that shows ratiometric UV changes and significant fluorescence changes, Tetrahedron 61 (2005) 9111-9117.

[29] S.H. Li, F.R. Chen, Y.F. Zhou, J.N. Wang, H. Zhang, J.G. Xu, Enhanced fluorescence sensing of hydroxylated organotins by a boronic acid-linked schiff base, Chem. Commun. (2009) 4179-4181.

[30] A.E. Hargrove, R.N. Reyes, I. Riddington, E.V. Anslyn, J.L. Sessler, Boronic acid porphyrin receptor for ginsenoside sensing, Org. Lett. 12 (2010) 4804-4807.

[31] K. Yum, J.H. Ahn, T.P. McNicholas, P.W. Barone, B. Mu, J.H. Kim, R.M. Jain, M.S. Strano, Boronic acid library for selective, reversible near-infra red fluorescence quenching of surfactant suspended single-walled carbon nanotubes in response to glucose, ACS Nano 6 (2012) 819-830.

[32] W.T. Wu, T. Zhou, A. Berliner, P. Banerjee, S. Zhou, Glucose-mediated assembly of phenylboronic acid modified CdTe/ZnTe/ZnS quantum dots for intracellular glucose probing, Angew. Chem. Int. Ed. 49 (2010) 6554-6558.

400 [33] P.F. Shen, Y.S. Xia, Synthesis-modification integration: one-step fabrication of boronic acid
401 functionalized carbon dots for fluorescent blood sugar sensing, Anal. Chem. 86 (2014) 5323-5329.
402 [34] Y.Y. Liu, J.W. Zhu, Y.M. Xu, Y. Qin, D.C. Jiang, Boronic acid functionalized aza-bodipy
403 (azaBDPBA) based fluorescence optodes for the analysis of glucose in whole blood, ACS Appl.
404 Mater. Interfaces 7 (2015) 11141-11145.
405 [35] L.F. Chang, X.W. He, L.X. Chen, Y.K. Zhang, Mercaptophenylboronic acid-capped Mn-doped ZnS
406 quantum dots for highly selective and sensitive fluorescence detection of glycoproteins, Sens.
407 Actautors B 243 (2017) 72-77.
408 [36] J. Wally, P.J. Halbrooks, C. Vonrhein, M.A. Rould, S.J. Everse, A.B. Mason, S.K. Buchanan, The
409 crystal structure of iron-free human serum transferrin provides insight into inter-lobe
410 communication and receptor binding, J. Biol. Chem. 281 (2006) 24934-24944.
411 [37] H.Y. Li, Z.M. Qian, Transferrin/transferrin receptor-mediated drug delivery, Med. Res. Rev. 22
412 (2002) 225-250.
413 [38] C.B. Lavery, M.C. Macinnis, M.J. Macdonald, J.B. Williams, C.A. Spencer, A.A. Burke, D.J.G.
414 Irwin, G.B. D'cunha, Purification of peroxidase from horseradish (Armoracia rusticana) roots, J.
415 Agric. Food Chem. 58 (2010) 8471-8476.
416 [39] H.F. Wang, Y. He, T.R. Ji, X.P. Yan, Surface molecular imprinting on Mn-Doped ZnS quantum dots
417 for room-temperature phosphorescence optosensing of pentachlorophenol in water, Anal. Chem. 81
418 (2009) 1615-1621.
419 [40] D.M. Gao, Z.P. Zhang, M.H. Wu, C.G. Xie, G.J. Guan, D.P. Wang, A surface functional
420 monomer-directing strategy for highly dense imprinting of TNT at surface of silica Nnanoparticles,
421 J. Am. Chem. Soc. 129 (2007) 7859-7866.

[41] L. Tan, K.C. Chen, C. Huang, R.F. Peng, X.Y. Luo, R. Yang, Y.F. Cheng, Y.W. Tang, A fluorescent turn-on detection scheme for α-fetoprotein using quantum dots placed in a boronate-modified molecularly imprinted polymer with high affinity for glycoproteins, Microchim. Acta 182 (2015) 2615-2622.

[42] F.F. Wang, J.Y. Wen, L.Y. Huang, J.J. Huang, J. Ouyang, A highly sensitive “switch-on” fluorescent probe for protein quantification and visualization based on aggregation-induced emission. Chem. Commun. 48 (2012) 7395-7397.

[43] L.F. Chang, X.W. He, L.X. Chen, Y.K. Zhang, A fluorescent sensing for glycoproteins based on the FRET between quantum dots and Au nanoparticles, Sens. Actuators B 250 (2017) 17-23.

[44] N. Kaura, N. Singha, B. McCaughana, J.F. Callanb, AND molecular logic using semiconductor quantum dots, Sens. Actuators B 144 (2010) 88-91.

[45] X. Wang, L. Qu, J. Zhang, X. Peng, M. Xiao, Surface-related emission in highly luminescent CdSe quantum dots, Nano Lett. 3 (2003) 1103-1106.

ACCEPTED MANUSCRIPT

Figure Captions:

Scheme 1 Schematic illustration of the preparation procedures for boronic acid polymer functionalized Mn-doped ZnS QDs.

Fig. 1 TEM images of the prepared QDs@MPS (A) and QDs@MPS@AAPBA (C); HRTEM images of QDs@MPS (B) and QDs@MPS@AAPBA (D).

Fig. 2 The XRD patterns of QDs, QDs@MPS and QDs@MPS@AAPBA (A); FT-IR of QDs, QDs@MPS and QDs@MPS@AAPBA (B); XPS of QDs@MPS@AAPBA (C); and FL spectra of QDs@MPS and QDs@MPS@AAPBA (D) (The inset shows a photograph of the QDs@MPS (a) and QDs@MPS@AAPBA (b) in 20 mM PBS (pH 9.0) under irradiated by 285 nm light).

Fig. 3 TRF (from bottom to top: 0.0, 0.1, 0.2, 0.3, 0.4, 0.5, 0.6, 0.7, 0.8, 0.9, 1.0, 1.5, 2.0, 3.0 μM) (A) and HRP (from bottom to top: 0.0, 0.1, 0.2, 0.3, 0.4, 0.5, 0.6, 0.7, 0.8, 0.9, 1.0, 1.5, 2.0 μM) (C) concentration dependent on fluorescent emission spectra of QDs@MPS@AAPBA in 20 mM PBS (pH 9.0). The corresponding plots of $\Delta F/F_0$ against the concentration of TRF (B) and HRP (D), respectively. Binding constants of QDs@MPS@AAPBA and glycoproteins were fitted according to the linear equation (inset of B) and (inset of D). The error bars represented the standard deviations of three independent experiments.

Fig. 4 $(F-F_0)/F_0$ of QDs@MPS@AAPBA in the presence of TRF, HRP or other analogues. The concentration of analyst is 1.0 μM for both TRF and HRP, 10 μM for BSA, CYT and LYZ, 100 μM for glucose and fructose, respectively (A). Change ratio $(F-F_0)/F_0$ of QDs@MPS@AAPBA upon the concentration of 1.0 μM TRF in the presence of background

461 particles of glucose (100 μM), Na^+ (142 mM), K^+ (5 mM), Mg^{2+} (2 mM) Ca^{2+} (3 mM), Cl^-

462 (100 mM) HCO_3^- (25 mM), BSA (10 μM), CYT (10 μM) and LYZ (10 μM).The amount of

463 QDs@MPS@AAPBA is 100 mg L^{-1} in 20 mM PBS (pH 9.0) (B).

464 **Fig. 5** The pH-dependent fluorescent intensity changes of QDs@MPS@AAPBA in the

465 presence and absence of 1μM TRF.

466

467

ACCEPTED MANUSCRIPT

468 **Scheme 1**

469

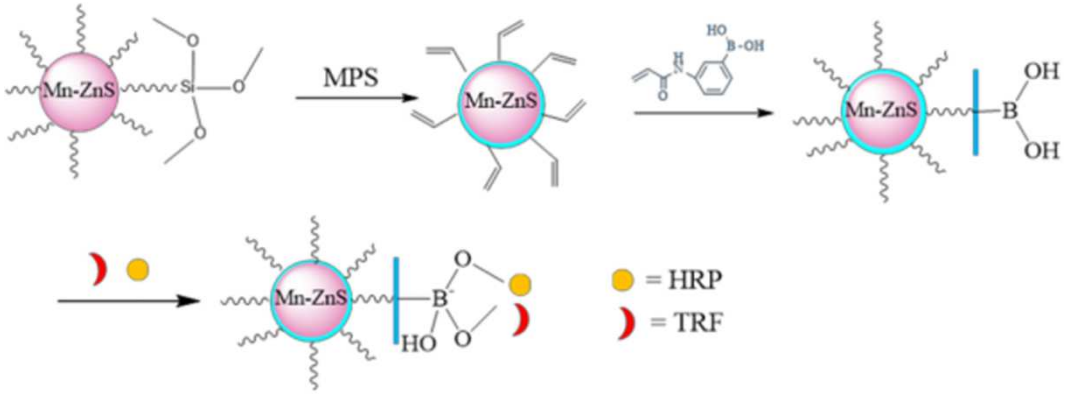

470

471

472

ACCEPTED MANUSCRIPT

473 **Fig. 1**

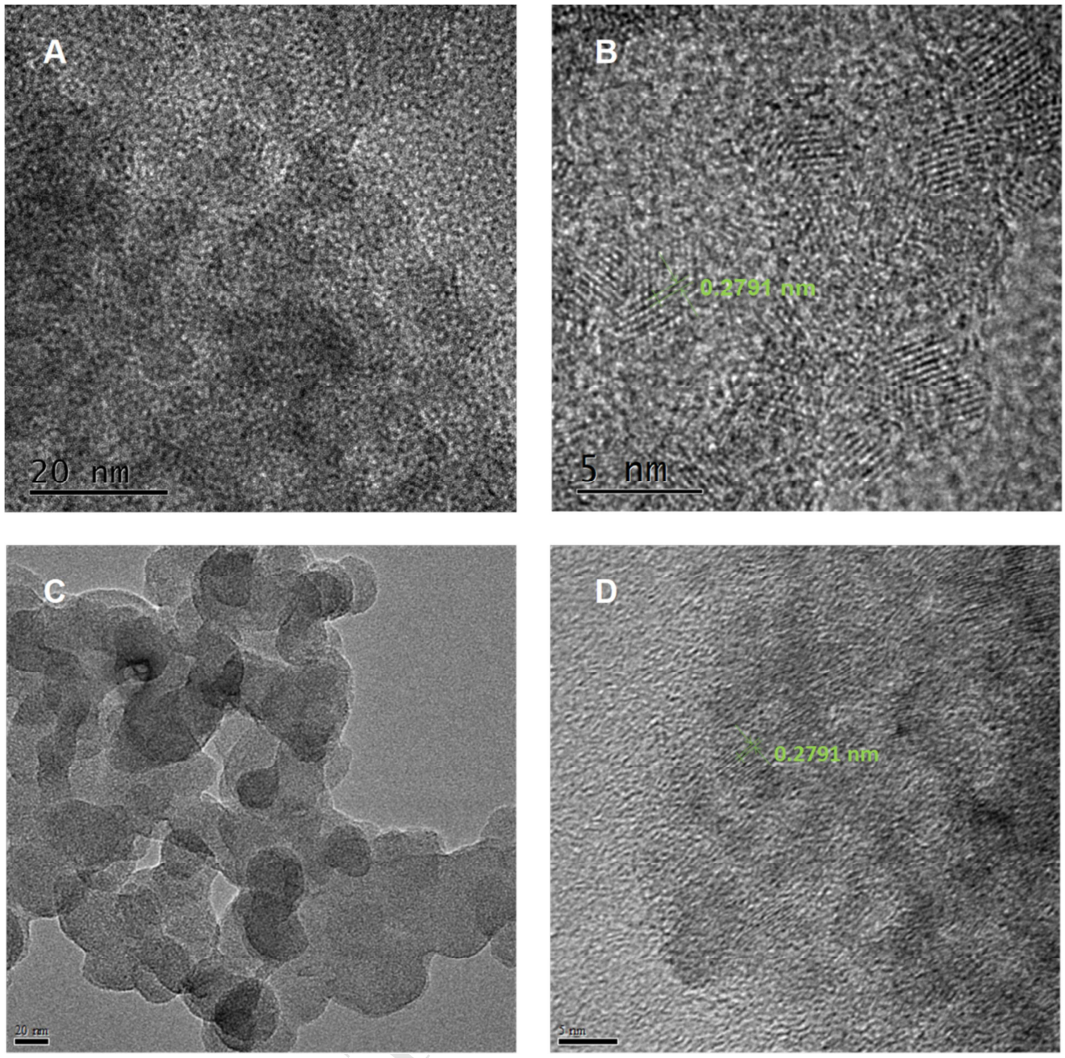

474

475

ACCEPTED MANUSCRIPT

476 **Fig. 2**

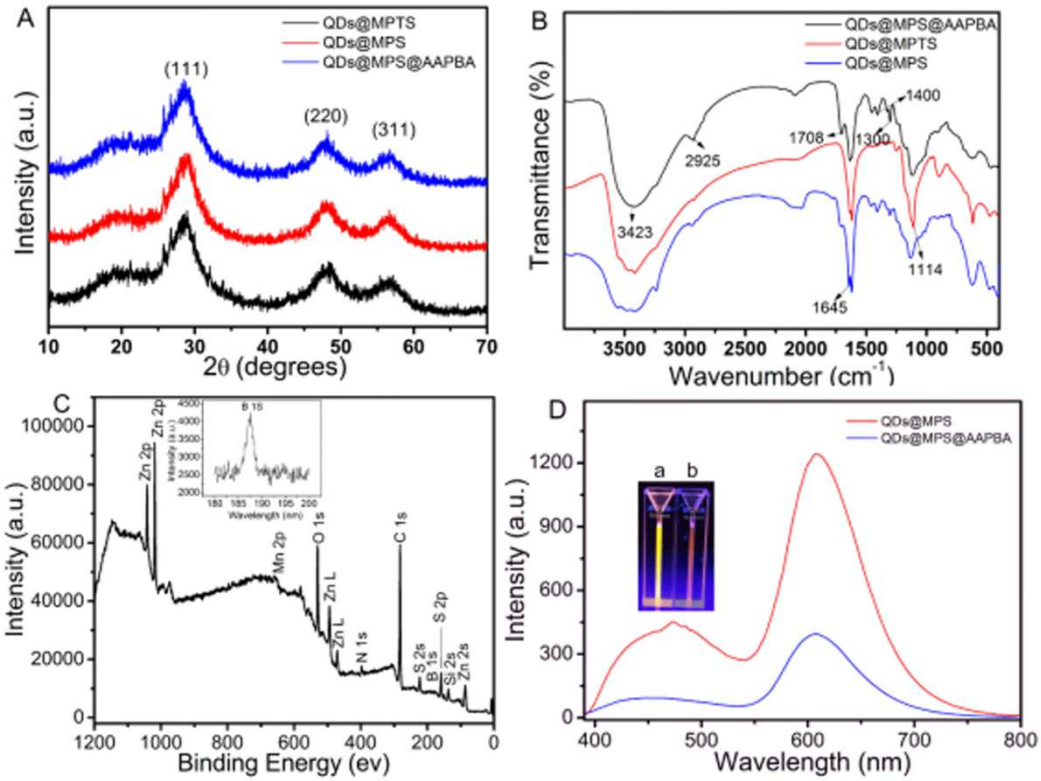

477

478

479

480

ACCEPTED MANUSCRIPT

481 **Fig. 3**

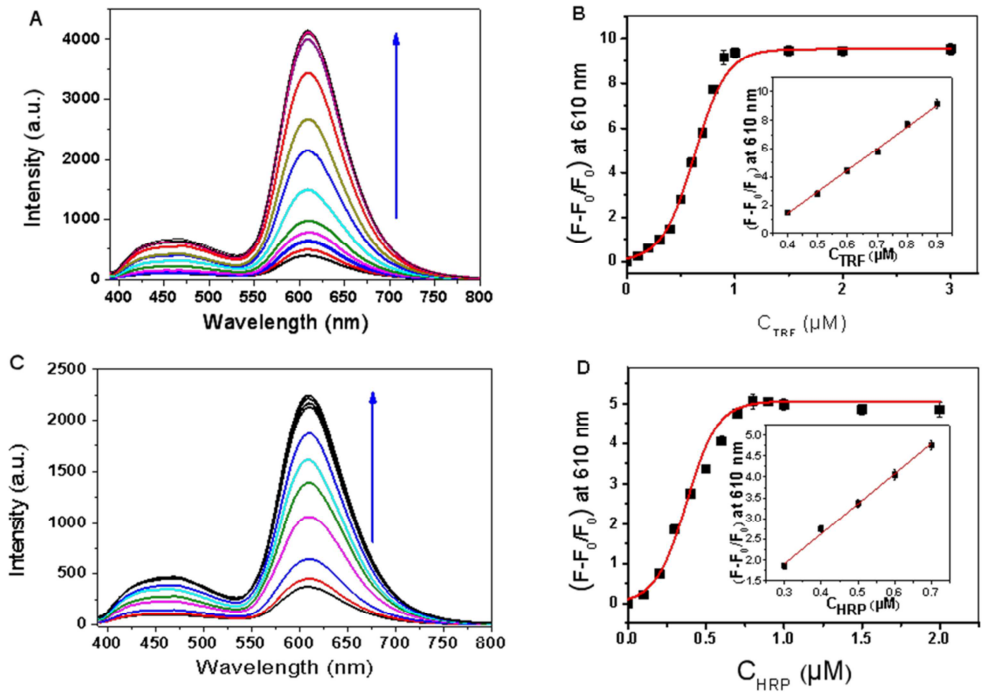

482

483

ACCEPTED MANUSCRIPT

484 **Fig. 4**

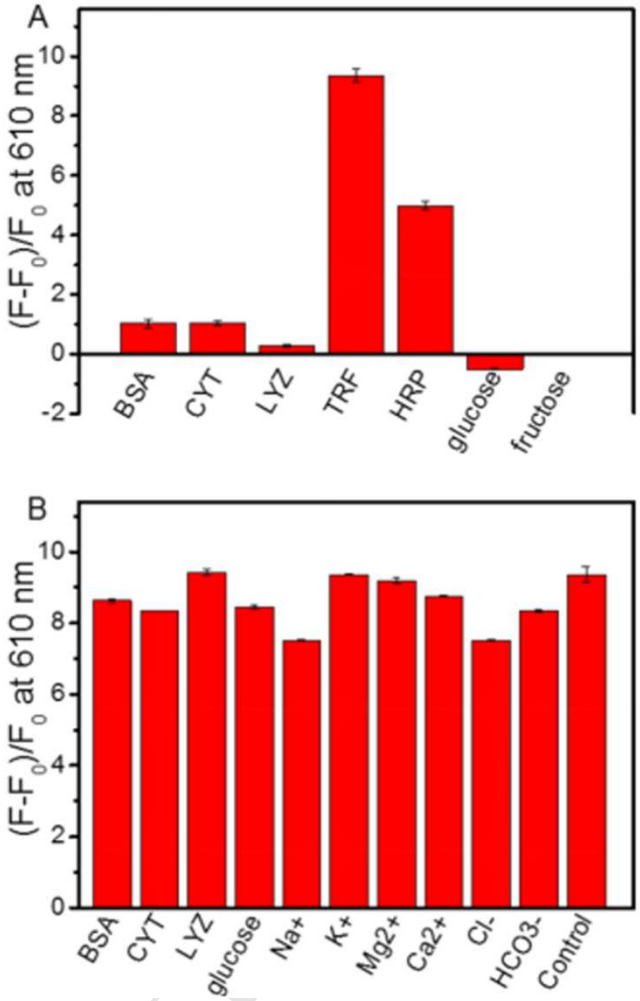

485

486

487

488

489 **Fig. 5**

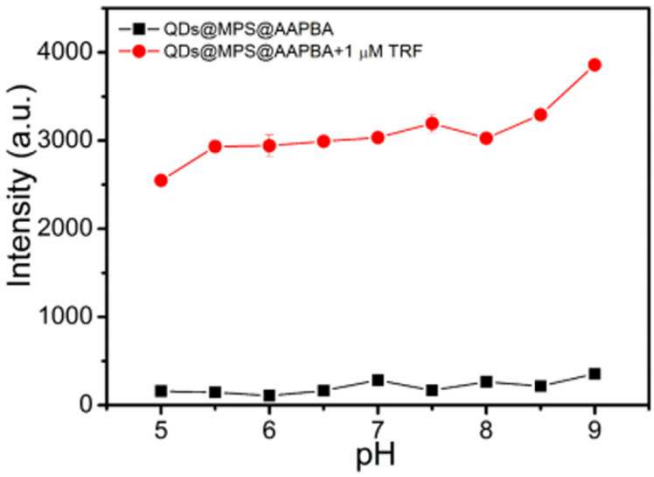

490

491

492

493

494

ACCEPTED MANUSCRIPT

495 **Table 1.** Comparison of the proposed method with the other reported methods for determination of
496 glycoproteins.

497

Method	Detection limit (nM)	[Refs.] 498
boronic acid quinoline modified $P_{GMA/EDMA}$ beads	2.6	[12]
APBA-Cu NCs	20	[21]
BSPA	10	[42]
MBA@QDs	5.69	[35]
QDs-AuNPs	0.94	[43]
QDs@MPS@AAPBA	0.14	This work

ACCEPTED MANUSCRIPT

499 **Table 2.** Recovery (mean±s; n=3) for the determination of TRF in the serum samples.

Samples	TRF spiked concentration (10^{-7} M)	TRF found concentration (10^{-7} M)	Recovery (%)
bovine serum 1	5.000	6.800±0.2	103.0±0.3
bovine serum 2	6.000	7.700±0.1	101.7±0.1
bovine serum 3	7.000	8.300±0.2	95.7±0.1
bovine serum 4	8.000	9.200±0.5	95.8±0.5

500

ACCEPTED MANUSCRIPT

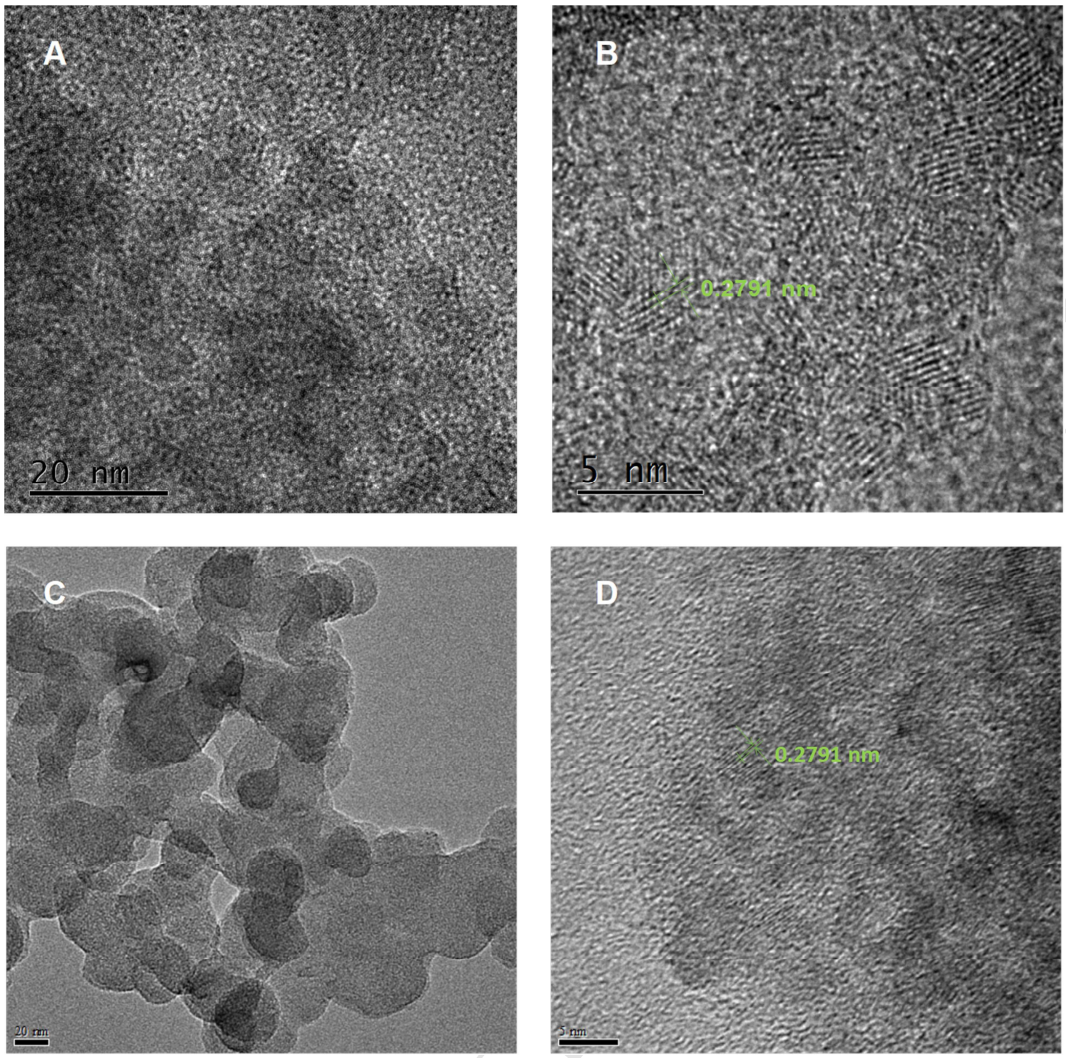

ACCEPTED MANUSCRIPT

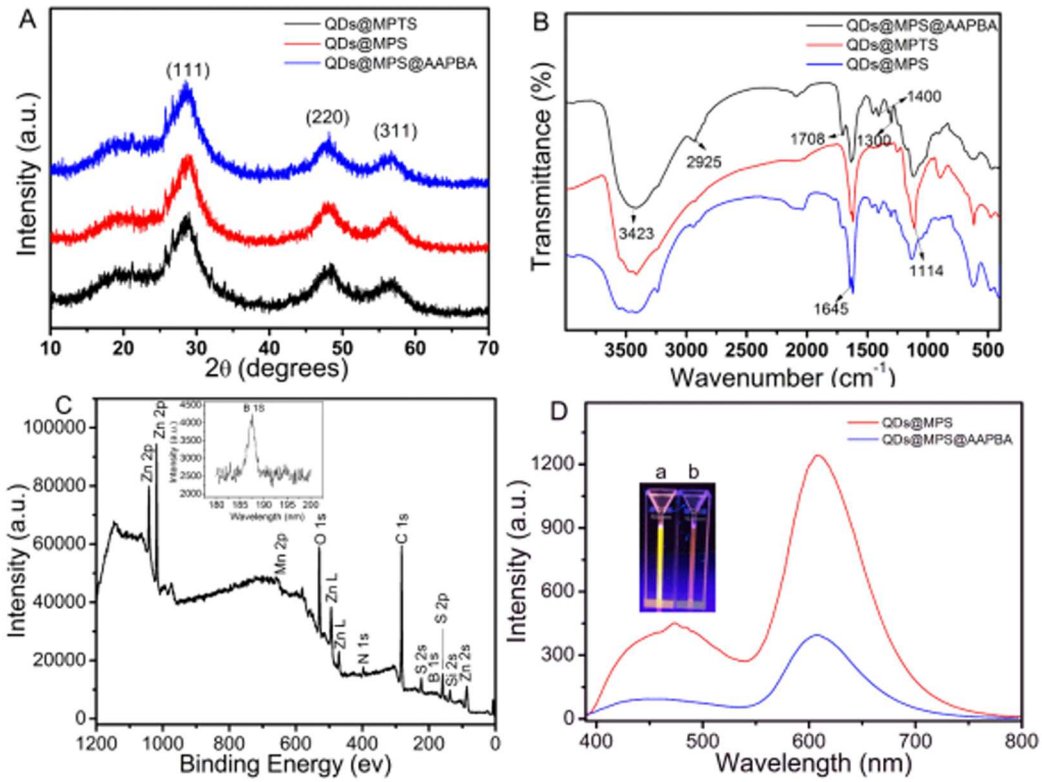

ACCEPTED MANUSCRIPT

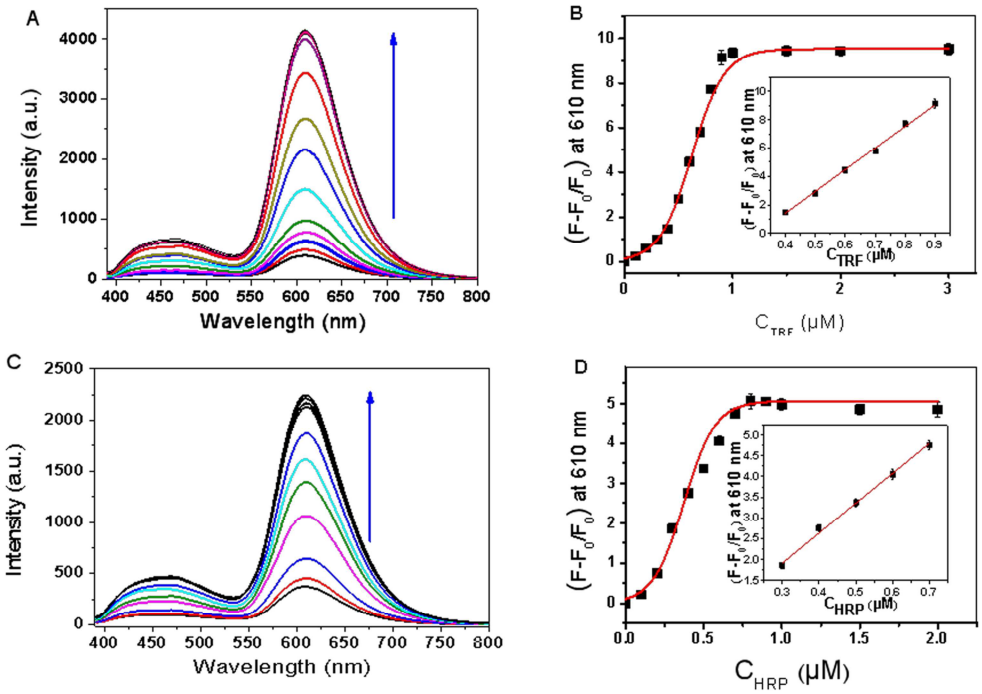

ACCEPTED MANUSCRIPT

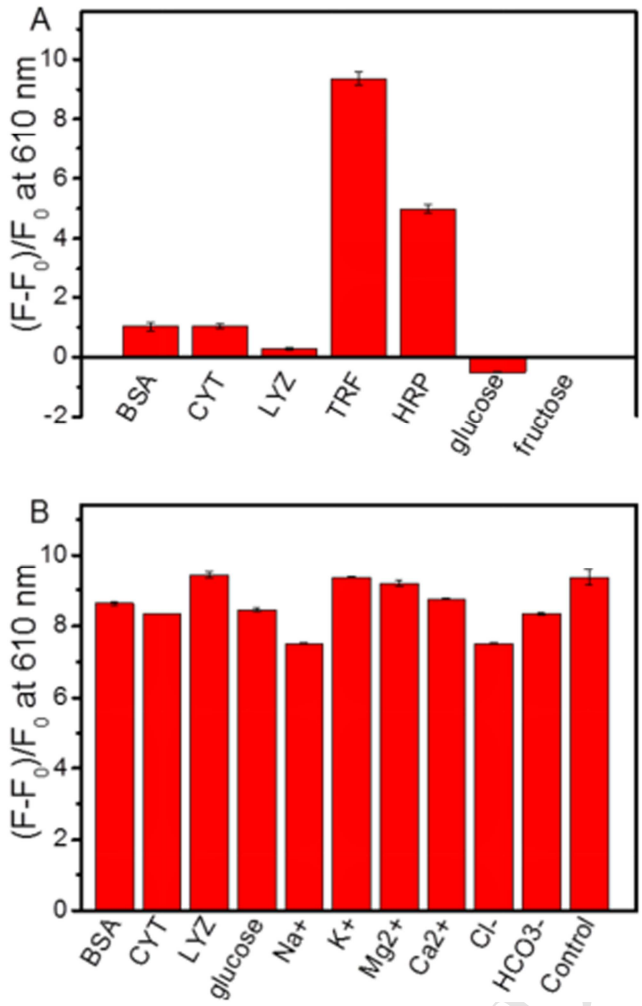

ACCEPTED MANUSCRIPT

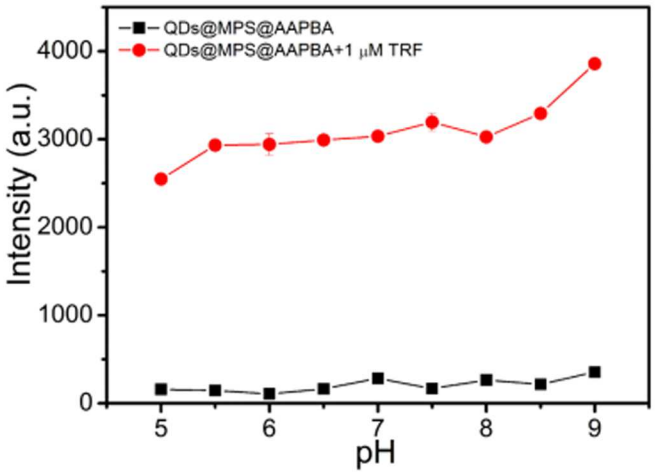

ACCEPTED MANUSCRIPT

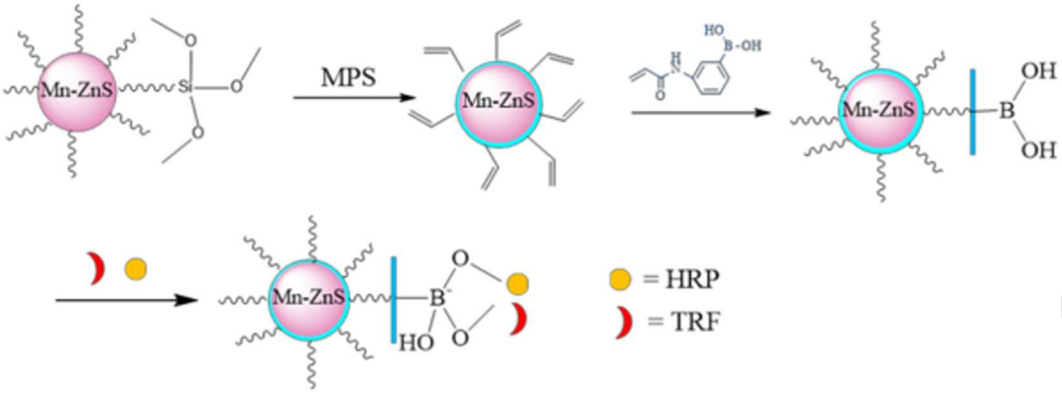

ACCEPTED MANUSCRIPT

ACCEPTED MANUSCRIPT

Highlights

- A simple fluorescence turn-on sensor based on boronic acid polymer capped Mn-doped ZnS quantum dots for the highly sensitive detection of glycoproteins.
- The limit of detection of the selected glycoproteins was lower than 0.1 nM.
- The sensor could be applied in a wide pH range of 5.0-9.0.
- High selectivity and anti-interference ability in TRF detection in serum.

ACCEPTED MANUSCRIPT